ORGANOMETALLICS

pubs.acs.org/Organometallics Article

Iridium and Palladium CO_2 Hydrogenation in Water by Catalyst Precursors with Electron-Rich Tetrazole Ligands

Edward Ocansey, James Darkwa, and Banothile C. E. Makhubela*

Cite This: https://dx.doi.org/10.1021/acs.organomet.0c00276 Read Online

ACCESS | Metrics & More | Article Recommendations | Supporting Information

ABSTRACT: Hydrogenation of CO_2 to formate serves as a means of H_2 storage. By utilizing robust, electron-rich and bulky N^N bidentate tetrazolylpyridyl ligands, we have prepared CO_2 hydrogenation iridium(III) and palladium(II) catalyst precursors (**3**−**7**) that operate in water as a solvent. *In situ* ^{1}H NMR spectroscopic data obtained when the hydrogenation catalyst is **5** detect that a hydrido-bridged binuclear iridium intermediate compound is formed prior to the formation of the catalytically active iridium hydride species. This hydrido-bridged iridium intermediate is observable by *in situ* ^{1}H NMR spectroscopy even after extended periods of storage. In addition, we demonstrate that product formation in the CO_2 hydrogenation, catalyzed by these tetrazolylpyridyl iridium catalysts, proceeds via either CO_2 hydrogenation or $NaHCO_3$ reduction.

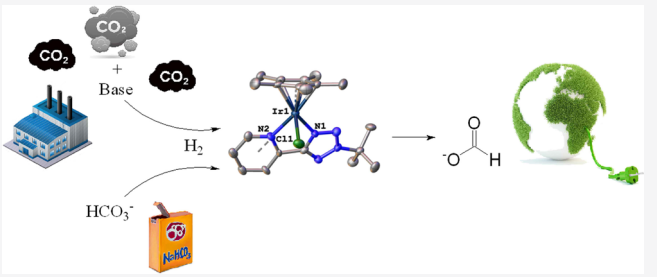

INTRODUCTION

Currently, the use of CO_2 as a carbon source in a variety of synthetic processes is receiving attention as a result of its abundance, nontoxicity, and low cost.[1] Homogeneous catalytic hydrogenation of CO_2 to various products such as formates, methanol, and dimethyl ether provides one approach to transform CO_2 into valuable chemicals. CO_2 is considered an environmental nuisance and a pollutant; as such, hydrogenating it serves as a means of storing hydrogen for other catalytic processes (such as in transfer hydrogenation) and molecular hydrogenation. Indeed, transfer hydrogenation reactions are of industrial importance, especially in the pharmaceutical, perfume, and agrochemical industries, where it has been shown to be an easy and safer way to work with hydrogen carriers (such as methanol, formic acid, and isopropyl alcohol) as opposed to molecular hydrogen.[2−4]

Several metals, such as iridium, ruthenium, palladium, and nickel, have been reported as catalysts with varying degrees of success for the hydrogenation of CO_2. The pioneering research by Inoue and co-workers with Ru, Rh, and Ir triphenylphosphine complexes as catalysts gave some of the first examples of CO_2 hydrogenation to formic acid.[5] They hydrogenated CO_2 to formic acid using a mixture of CO_2 and H_2 (2.5 MPa/2.5 MPa), the catalyst precursor, and a base at room temperature. Since then, other metals such as Pd and Ni, as either homogeneous or heterogeneous catalysts, have been used in CO_2 hydrogenation. In addition, relatively cheaper metals, such as Mn and Fe, can catalyze CO_2 hydrogenation.[6,7]

However, it is not only the metal in the catalysts that is effective in the hydrogenation; the nature of the ligand also has an effect on the catalysis. For example, Weilhard et al.[8] reported highly active Ru catalysts for CO_2 hydrogenation that make use of the synergistic effect of imidazolium-based ionic liquids with their associated acetate anions, which act as an acid buffer and stabilizer for the catalytically active Ru−H species.

Generally homogeneous catalysts with phosphine ligands are effective for a variety of catalytic reactions.[9−11] For example, Milstein and co-workers have reported a P^N^P iron(II) dihydride pincer complex that was utilized as a catalyst for CO_2 hydrogenation. This catalyst is able to catalyze the hydrogenation of both CO_2 and $NaHCO_3$ to formate with TONs ranging between 300 and 800, on par with those of other noble-metal catalysts, even with a low catalyst loading (0.1 mol %) and short reaction times (ca. 5−16 h).[12] Similarly, the Nozaki group has reported a (2,6-bis-(diisopropylphosphinomethyl)pyridine)iridium(III) trihydride complex that performs remarkably in hydrogenating CO_2 under basic aqueous conditions.[13] Even with a 1/1 CO_2/H_2 mixture and 5 MPa pressure at 200 °C, the Nozaki catalyst shows remarkable activity (i.e., TOF = 150000 h^{-1} in 2 h).[13] Another (P^N)iridium complex that has excellent catalytic activity (TON = 348000) is ((diisopropylphoshinoethyl)-amine)iridium(III) hydride, reported by Hazari and co-workers.[14] The ligand in this catalyst has an N−H group in the secondary coordination sphere of the iridium complex.

Received: April 22, 2020

Scheme 1. Synthesis of Ligands and Metal Complexes

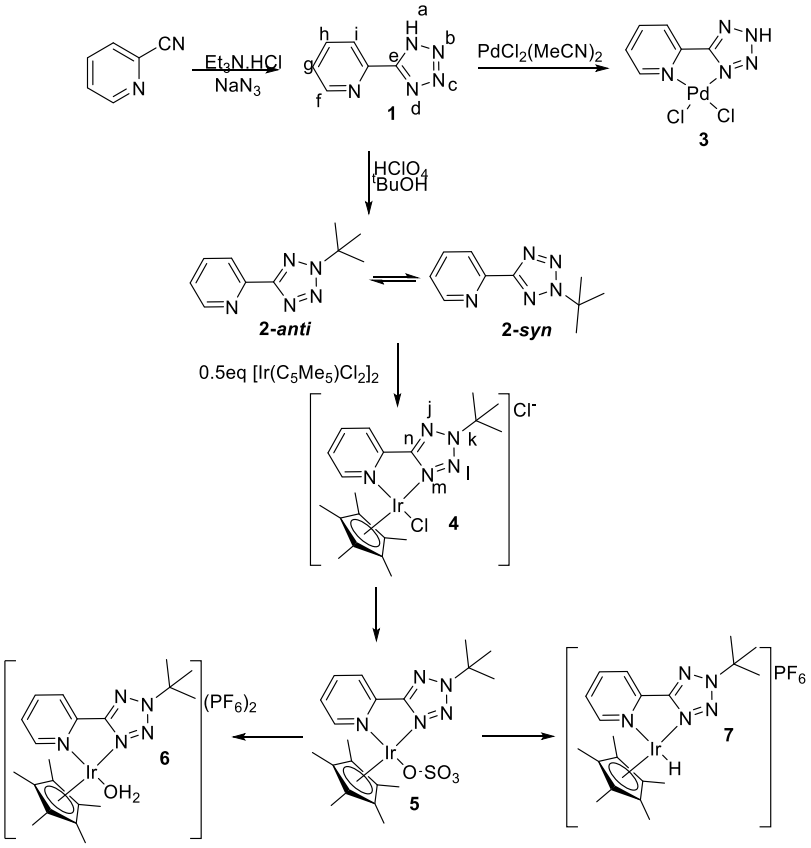

Thus, the excellent catalytic activity is attributed to H bonding between the N−H group in the ligand and CO_2, which thereafter undergoes reductive elimination to produce the catalytically active iridium hydride species. Computational evaluation of the catalytic system indicated that CO_2 insertion could happen more readily in the catalytic system, since it is easily stabilized by bridging via hydrogen bonding with the outer-sphere N−H group.[14]

In addition to the effect of ligands on catalytic activity, the nature of the solvent used for this reaction has also been shown to affect the catalytic activity. This is because catalytic intermediates can be stabilized by solvents or such solvents may influence the entropy differences between the reactants and products via solvation.[5] For instance, we recently utilized ruthenium(II) and iridium(III) half-sandwich complexes as catalysts for the CO_2 hydrogenation using a variety of solvents which suggested a solvent-dependent hydrogenation of CO_2, with THF/H_2O being an ideal solvent mixture.[15,16]

Generally, phosphine ligands are mostly air and moisture sensitive in catalytic systems for CO_2 hydrogenation, and so nonphosphine ligands, such as N^N and N^C ligands, have also been studied to good effect. For example, the Himeda group has observed the generation of CO_2/H_2 in the course of transfer hydrogenation of ketones with the half-sandwich complex [Cp*Rh(bpy)Cl]Cl in aqueous solutions of formic acid. They then later noticed that the Rh complex could also catalyze CO_2 hydrogenation in water.[17] This observation then led to the synthesis of the series of half-sandwich complexes $[(C_nMe_n)M(4,4'\text{-}R_2\text{-}bpy)Cl]^+$ (n = 5, 6; M = Ir, Rh, Ru; R = OH, OMe, Me, H) for the hydrogenation of CO_2. In this study, complexes containing hydroxyl groups were found to be very responsive to protonation and deprotonation of the hydroxyl substituents at different pHs. This led to a class of compounds referred to as "proton-responsive ligands", which have tunable electronic properties at different pHs and which greatly improve their ability to catalyze CO_2 hydrogenation. Indeed, the Himeda water-soluble Ir(III) complex $[Cp^*Ir(6,6'\text{-}R_2\text{-}bpy)(OH_2)]SO_4$ (bpy = 2,2′-bipyridine, R= OH) is able to demonstrate the role "proton-responsive ligands" play in activating CO_2 via electronic and second-sphere coordination effects.[18] As a result of this, they were able achieve high catalytic activity (TON = 24000) in CO_2 hydrogenation at ambient temperatures and pressures. A strong correlation between hydrogen (H^-), methyl, methoxy, and hydroxy substituents on the bipyridine ring in the catalysts and the catalytic activities, as a result of electronic effects, was also demonstrated. They thus proposed a mechanism that involves the generation of active Ir−H species, assisted by the pendant base O^- in the catalyst. These oxyanion groups are electron-rich and contribute to H_2 cleavage, while they play stablilizing roles in various intermediates. The role of the oxyanion was proven experimentally by NMR experiments and by DFT calculations.[18] A similar observation of O^--assisted H_2 cleavage leading to efficient CO_2 hydrogenation by bidentate (pentamethylcyclopentadienyl)iridium(III) pyridine-diazole catalysts (TON = 11000)[19] under mild reaction conditions of temperature (50 °C) and pressure (1 MPa CO_2/H_2 1/1) was reported. Here, the catalyst precursors contain a hydroxyl and uncoordinated NH functional groups that are responsible for the "proton-responsive" behavior.[19]

Tetrazole-containing compounds have recently found applications in CO_2 capture, having been used as linkers in

https://dx.doi.org/10.1021/acs.organomet.0c00276
Organometallics XXXX, XXX, XXX−XXX

metal−organic frameworks (MOFs).[20] In addition, tetrazole-stabilized catalyst precursors have served as sources of electron-rich N atoms, which contribute toward improved catalytic activity at the metal center in hydrogenation reactions.[18] It is the ability of tetrazole-containing compounds to capture and possibly activate CO_2 that led to the present study. We designed new electron-rich half-sandwich (tetrazolylpyridyl)iridium(III) and (tetrazolylpyridyl)-palladium(II) chloride complexes, with the potential to exhibit "proton responsiveness" at the N2 position of the tetrazole ring, and investigated their ability as catalysts for CO_2 hydrogenation.

RESULTS AND DISCUSSION

Synthesis and Characterization of the Tetrazole-Based Ligands. The synthesis of compound **1** was achieved by first reacting 2-cyanopyridine with a slight excess of NaN_3 in the presence of excess $Et_3N{\cdot}HCl$ (Scheme 1). Compound **1** was then isolated after adding a solution of HCl to precipitate the product as an air- and moisture-stable brown solid in excellent yield. Compound **1** is soluble in most organic solvents and was characterized by NMR spectroscopy and elemental analysis. The ^1H NMR spectrum of **1** showed only a slight downfield shift of about 0.1−0.2 ppm in comparison to the ^1H NMR spectrum of 2-cyanopyridine.

Alkylation of **1** with *tert*-butyl alcohol (Scheme 1) resulted in the formation of 2-*tert*-butyl-5-(2-pyridyl)-2*H*-tetrazole (**2**). Compound **2** was obtained as a white solid in good yield (77%) and is soluble in organic solvents but insoluble in water. The key ^1H NMR peak of **2** is at 1.8 ppm, integrating for nine protons, confirming that the alkylation of **1** had occurred. In fact, selective alkylation of the two nitrogen atoms b and c in **1** is possible in the presence of a strong acid, because on protonation of the nitrogen atoms of the pyridine the d nitrogen of **1** should result in the delocalization of charge among nitrogens a, e, and d (Scheme 1). This would lead to two equivalent nitrogens (i.e., b and c) as available sites for the alkylating agent to attack.[21] It is also interesting to note that due to rotation along the C−C bond between the pyridine and tetrazole rings, compound **2** can exist as rotamers. Indeed, quantum mechanical calculations have shown that in DMSO and DMF the total energy of **2**-*syn* is only about 1 kJ mol^{-1} lower than that of **2**-*anti*.[22]

Synthesis of Tetrazolyl Palladium and Iridium Complexes. The synthesis of the new palladium complex **3** (Scheme 1) was achieved by reacting a dichloromethane solution of compound **1** with $[PdCl_2(MeCN)_2]$ in a 1/1 ratio. Complex **3** precipitated out of solution as a yellowish solid in good yield and is partially soluble in chloroform but completely soluble in DMSO. The ^1H NMR spectrum of **3** showed only slight shifts in proton signals of 0.1−0.2 ppm in comparison to the ^1H NMR spectrum of **1**. For example, proton f (Scheme 1) shifted downfield by about 0.1 ppm while proton h shifted downfield by about 0.2 ppm and proton i shifted upfield by about 0.2 ppm, and there were no observed shifts in the signal of g.

Interestingly, the reaction of compound **1** with $[Ir(C_5Me_5)Cl_2]_2$ in a 2/1 ratio resulted in an immediate loud sound accompanied by the violent ejection of the septum that was used to seal the Schlenk tube in which the reaction was run. We suspect this was the result of the detonation of the tetrazole to give off molecular nitrogen,[23] possibly from stirring of the reaction mixture. There were no further reactions of **1** undertaken with the iridium precursor, and when reactions were performed with compound **2** and the iridium precursor, *caution was taken by connecting the Schlenk tube to a vacuum line in order to release any built-up pressure and also minimize agitation in the initial stages of the reaction*. Synthesis of the iridium complex **4** (Scheme 1) was achieved by reacting compound **2** with $[Ir(C_5Me_5)Cl_2]_2$ in a 2/1 ratio in dichloromethane. Compound **4** was obtained in pure form as a yellow solid in quantitative yield after the solvent was removed *in vacuo*. The ^1H NMR spectrum of **4** indicated more significant shifts downfield in the proton signals of about 0.4−0.8 ppm, especially for the pyridinyl protons, in comparison to the ^1H NMR peaks of **2**. In contrast to compound **2**, there was no indication from the ^1H NMR spectrum that **4** had rotameric forms, since the spectrum of *N*-k-*tert*-butyl-substituted iridium complex **4** (i.e., the **2**-*anti* form) is expected to be different from the ^1H NMR spectrum of *N*-l-*tert*-butyl-substituted iridium complex **4** (i.e., the **2**-*syn* form). Indeed, ^1H NMR data show the product to be the sterically hindered *N*-k-*tert*-butyl-substituted iridium complex **4**.

Reaction of **4** with Ag_2SO_4 as a halide abstractor in water yielded a sulfato complex, **5**, instead of the expected iridium aqua complex, **6**. This is in contrast to various reports of halide abstraction from $[(N^\wedge N)Ir(Cl)]$ complexes with Ag_2SO_4 in water that produce the corresponding aqua complexes $[(N^\wedge N)Ir(OH_2)]^+$.[24] For most iridium chloro complexes, halide abstraction in water leads to cationic iridium aquo species. However, a (N^N)iridium sulfato complex formed following chloride abstraction from the (N^N)iridium chloro starting material, using Ag_2SO_4 as reported in the literature supports the formation of **5** from **4**.[25] Formation of the iridium aqua complex **6** was eventually achieved by reaction of the iridium sulfato complex **5** with KPF_6 in water. The formation of both iridium complexes **5** and **6** was confirmed by ^1H NMR spectroscopy. In addition, the $^{13}P\{^1H\}$ NMR of **6** with peaks around −143 ppm confirmed the presence of the PF_6 counterion. Further support for the formation of **5** and **6** was provided by mass spectrometry, for which m/z $[M + H]^+$ 628.1513 and $[M]^+$ 550.1962 were observed for **5** and **6**, respectively. The reaction of complex **5** with HCOONa, followed by a counterion exchange with $NaPF_6$, resulted in the formation of the iridium hydride species **7**. The presence of the hydride ligand was confirmed by a ^1H NMR signal peak around −11 ppm that integrates for one proton (Figure SI-1). Similarly, the $^{13}P\{^1H\}$ NMR spectrum (Figure SI-1) with peaks at around 140 ppm confirmed the presence of the PF_6 counterion in complex **7**. Complexes **5**−**7** are all soluble in DMSO; however, only **5** is soluble in water.

Single Crystal X-ray Structure of Complex 4. Yellow single crystals of **4** were grown by slow evaporation of the complex in dichloromethane. Crystallographic data and the molecular structure of this complex are shown in Table 1 and Figure 1. Complex **4** crystallizes in the monoclinic space group *C*2/*c* with a piano-stool geometry (Figure 1). As expected, the iridium−N(pyridine) bond distance (2.146(7) Å) is longer than that of the iridium−N(tetrazole) bond (2.078(7) Å). This suggests a stronger iridium−N(tetrazole) bond in comparison to the iridium−N(pyridine) bond. This is possibly as a result of delocalization of the several lone pairs of the nitrogens in the tetrazole ring, resulting in enhanced electron donation to the iridium center and hence a shorter Ir−N bond length. The bond lengths between iridium and the donating ligands as well as the bond angles are in conformity with

https://dx.doi.org/10.1021/acs.organomet.0c00276
Organometallics XXXX, XXX, XXX−XXX

Table 1. Crystal Data and Structure Refinement Details for Complex 4

empirical formula	$C_{20}H_{28}N_5Cl_2Ir$
formula wt	601.14
temp/K	100
cryst syst	monoclinic
space group	$C2/c$
a/Å	33.847(7)
b/Å	9.694(2)
c/Å	16.767(4)
α/deg	90
β/deg	119.082(4)
γ/deg	90
V/Å^3	4808.1(17)
Z	48
ρ_{calcd}/g cm^{-3}	1.6504
μ/mm^{-1}	5.796
$F(000)$	2217.2
cryst size/mm^3	0.3 × 0.2 × 0.2
radiation	Mo Kα (λ = 0.71073)
2θ range for data collection/deg	2.76−56.76
index ranges	$-45 \le h \le 44$, $-12 \le k \le 12$, $-22 \le l \le 22$
no. of rflns collected	77162
no. of indep rflns	6017 (R_{int} = 0.2239, R_σ = 0.1067)
no. of data/restraints/params	6017/0/267
goodness of fit on F^2	1.004
final R indexes ($I \ge 2\sigma(I)$)	R1 = 0.0563, wR2 = 0.1293
final R indexes (all data)	R1 = 0.0942, wR2 = 0.1513
largest diff peak, hole/e Å^{-3}	3.94, −2.27

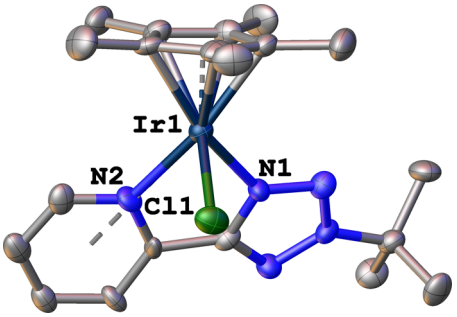

Figure 1. Molecular structure of complex **4**. Hydrogen atoms, the Cl counterion, and residual solvents are omitted for clarity. Selected bond distances (Å) and bond angles (deg); Ir(1)−Cl(1) 2.394(2), Ir(1)−N(1) 2.078(7), Ir(1)−N(2) 2.146(7); N(1)−Ir(1)−Cl(1) 88.3(2), N(2)−Ir(1)−N(1) 75.0(3).

several iridium N^N bidentate complexes that have been reported in the literature.[26−28]

A space-filling model of **4** showing the electrostatic potential map indicates the highly electron rich site is found at the iridium center due to electron donation from the Cp* and the pyridyl-tetrazole donor sites in **4**. In addition, N2 in the tetrazole ring is fairly electron rich (Figure 2), which suggests that it is possibly available to act as a "proton-responsive" site during the catalytic cycle of CO_2 hydrogenation.

Optimization of CO_2 Hydrogenation Reaction Conditions Using 4. When CO_2 hydrogenation was carried out using **4** as a catalyst precursor in either ethanol or DMSO as the solvent, there was only a marginal amount of formate produced with a TON of around 40 (Figure 3). When water was used as the solvent, TONs almost doubled to around 80

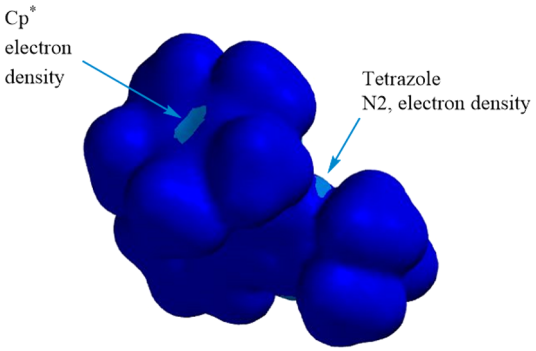

Figure 2. Electrostatic potential map of **4**.

(Table SI-T1). This indicated that water plays a crucial role in the process during the CO_2 hydrogenation reaction. Water may serve as a labile ligand which stabilizes various reaction intermediates during the catalytic reaction. In addition, water could contribute toward increasing reaction rates by facilitating hydrogen bonding between the generally accepted catalytically active iridium hydride species and oxygen atoms present in CO_2.[19]

This observation was further noticed when a water/THF mixture (4/1) was used, which resulted in a drop in TONs. As expected, increasing the temperature from 120 to 160 °C also resulted in an increase in formate production and the corresponding TONs. Changing the base from KOH to DBU did not result in a significant change in TON; however, using the weak base triethylamine resulted in a drop in TONs. Using an equimolar amount of K_2CO_3 resulted in an increase in TON, possibly as a result of an increase in the amount of potassium ions present in solution. A higher concentration of K^+ readily stabilizes any formate present, resulting in increased formate generation. Reducing the amount of CO_2 with respect to H_2 resulted in an increase in TON, with the optimum ratio being determined as a 1/2 CO_2/H_2 mixture. Reducing the reaction time from 24 to 18 h resulted in a drop in both the amount of formate and TON; however, lowering the catalyst loading to 1 μmol resulted in a significant drop in the amount of formate formed but an increased TON. Representative ^1H and $^{13}C\{^1H\}$ NMR spectra after CO_2 hydrogenation reaction using **4** are shown in Figure 4.

Precatalysts **3** and **5**−**7** were also used for the CO_2 hydrogenation under reaction conditions identical with those used for **4**. This was done to evaluate the effect of different metals as well as the various coligands (hydride, aqua, sulfato) (Table 2). All five precatalysts were used to run the hydrogenation reaction in the presence of mercury and in each instance gave slightly lower TONs (Table 2) in comparison to the reactions without mercury, signifying that the active catalysts in all cases were largely homogeneous. Precatalyst **3** is the least active (TON = 91; Table 2, entry 1), while complex **7** is the most active (TON = 561; Table 2, entry 5). This is expected, as the other iridium precatalysts (**4**−**6**) would have to generate the iridium hydride species *in situ* before catalyzing the CO_2 hydrogenation reaction. However, it is interesting to note that the aqua complex **6** was slightly more active than the sulfato complex **5**. This suggests that the formation of an iridium aqua species may be an important intermediate in the catalytic process. The reaction mixtures at the end of the hydrogenation showed a peak at 160 ppm in the $^{13}C\{^1H\}$ NMR spectra of these mixtures, assignable to a

https://dx.doi.org/10.1021/acs.organomet.0c00276
Organometallics XXXX, XXX, XXX−XXX

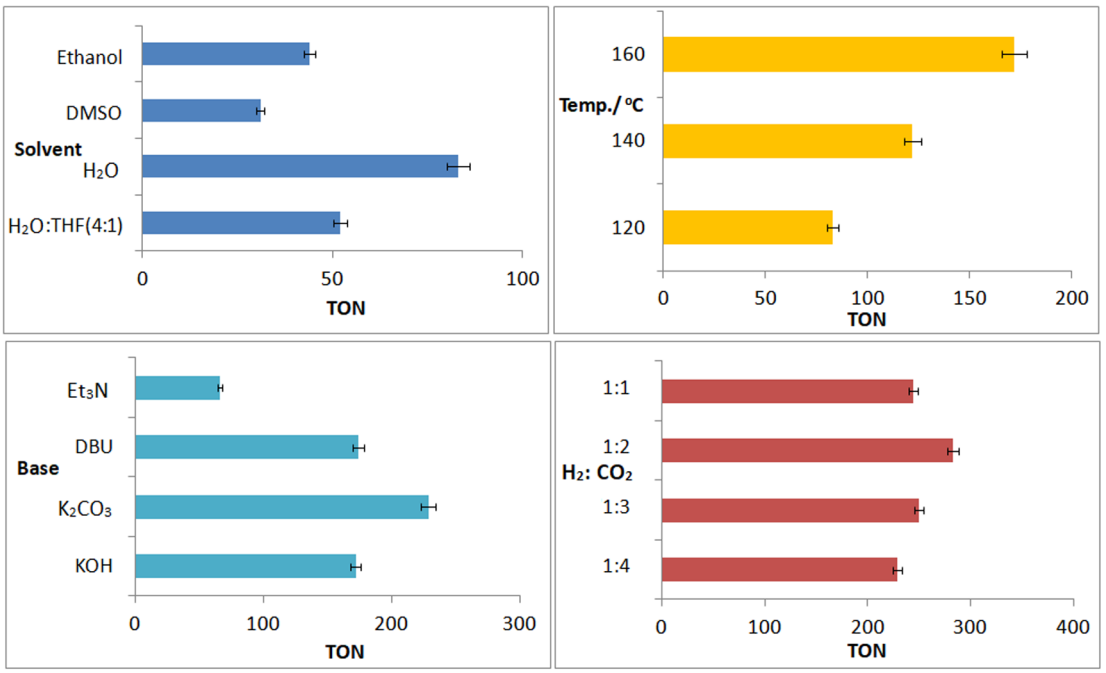

Figure 3. Optimization of reaction conditions using **4**. The reactions were performed in 10 mL of the appropriate solvent (or mixture) and 3.55 mmol of base at the appropriate temperature and total pressure (50 bar) with stirring (1500 rpm) in the presence of complex **4** (μmol) for 24 h using DMF as a standard. TON = (calculated mmol of $[HCO_2^-]$)/(mmol of catalyst).

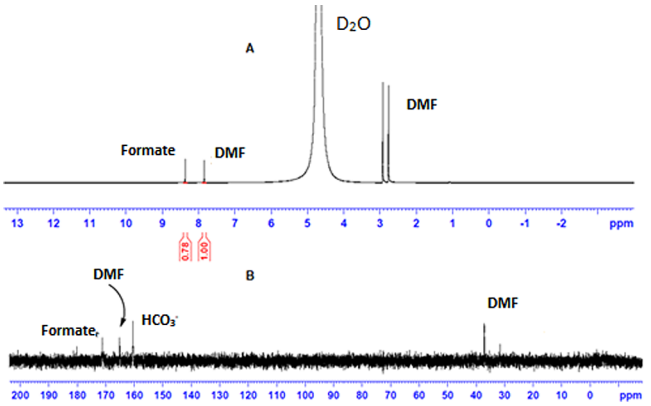

Figure 4. Typical (A) ^{1}H NMR spectrum and (B) $^{13}C\{^1H\}$ NMR spectrum of the contents of the reaction mixture after the CO_2 hydrogenation reaction using DMF as an internal standard.

bicarbonate ion (Figure SI-3). This suggested that the actual species undergoing hydrogenation are bicarbonate ions formed in solution from a combination of both CO_2 and K_2CO_3. Such a hydrogenation of bicarbonate ions has been reported in the literature.[29] In addition, CO_2 has been shown to exist in a variety of forms in aqueous solution in the presence of carbonate ions.[30] In order to confirm this, the hydrogenation reaction was carried out with K_2CO_3 but without CO_2 (Table 2, entry 6). The product from this reaction was formate but at reduced TON, confirming the participation of the carbonate ion in the CO_2 hydrogenation when K_2CO_3 is used as the base. The catalytic activities of **4**–**7** in comparison to those of similar N^N bidentate azole iridium Cp* precatalysts[19] are inferior. However, the amount of product formed for these N^N bidentate azole iridium Cp* precatalysts[19] was lower in comparison to **4**–**7**. Thus, higher TONs at a lower catalyst

Table 2. Evaluating Precatalysts 3–7 for CO_2 Hydrogenation[a]

entry	catalyst	product (product[c])/mmol	$[HCO_2^-]$/mM	TON (TON[d])
1	**3**	0.45 (0.39)	45	91 (78)
2	**4**	1.42 (1.32)	142	283 (264)
3	**5**	1.97 (1.80)	197	396 (360)
4	**6**	2.16 (1.88)	216	433 (376)
5	**7**	2.80 (2.02)	280	561 (403)
6	**4**	0.58[b]	58	116
7	[Cp*Ir(L1)(Cl)]Cl[e]	0.26	26	1300
8	[Cp*Ir(L2)(Cl)]Cl[e]	0.91	91	4600

[a]Reaction conditions unless indicated otherwise: performed in 10 mL of H_2O and 3.55 mmol of K_2CO_3 at 160 °C under 50 bar of CO_2/H_2 (1/2) with stirring (1500 rpm) in the presence of a complex (5 μmol) for 24 h. [b]Reaction carried out in the presence of only 33 bar of H_2. [c]Calculated amount of $[HCO_2^-]$ in the presence of excess mercury. [d]Calculated TON of $[HCO_2^-]$ when the reaction was carried out in the presence of excess mercury. [e]Reference 19: L1 = 2-(1*H*-imidazol-2-yl)pyridine, L2 = 2-(1*H*-pyrazol-3-yl)pyridine. The reactions were performed in 10 mL of a 2.0 M $KHCO_3$ aqueous solution (pH 8.5) at 50 °C under 1.0 MPa of H_2/CO_2 (1/1) with stirring (1500 rpm) in the presence of a complex (20 μm) for 24 h.

loading do not necessarily translate to higher TONs at increased catalyst loading. It has to be noted that, for these N^N bidentate azole iridium Cp* precatalysts,[19] the increased activity is attributed to the presence of proton-responsive groups on the ligands. As such, it could be reasonably expected that the activity of **4**–**7** may be improved by introducing proton-responsive groups.

Proposed Mechanism for the Iridium-Catalyzed CO_2 Hydrogenation. When **5** was reacted with H_2 in DMSO-d_6,

https://dx.doi.org/10.1021/acs.organomet.0c00276
Organometallics XXXX, XXX, XXX–XXX

the new iridium species **B** was observed, as evidenced by its ^{1}H NMR spectrum, which displayed a peak at around −14 ppm (Figure SI-4). If **B** were the molecular hydrogen complex, doubling of the tetrazole aromatic peaks would be seen, as was reported for a similar N^N bidentate Cp* iridium dihydrogen complex (where the N^N bidentate ligand was an imidazole).[31] However, the ^{1}H NMR spectrum of **B** showed no such doubling of the tetrazole aromatic peak signals. In addition, since the dihydrogen iridium complex is expected to be very acidic, it should undergo facile deprotonation in water in order to yield **7**.[32] However, this was not observed when **B** was kept in a water solution containing DMSO-d_6 (Figure 5).

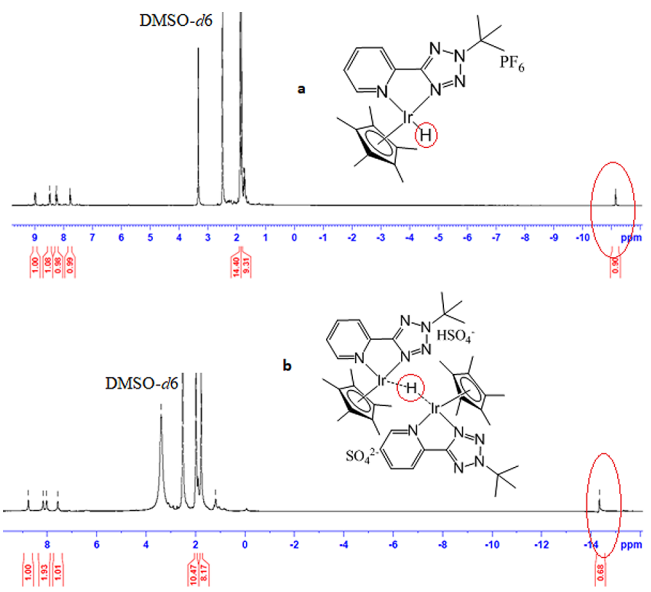

Figure 5. ^{1}H NMR spectra of (a) **7** and (b) intermediate **B**.

We have proposed the structure of **B** to be a hydrido-bridged iridium dinuclear species containing an Ir···H···Ir bond (Figure 5). In addition, the hydride signal of **B** is upfield in comparison to that of **7** (−11 ppm). This implies that the hydride in **B** is more hydridic (in this case being bonded to two iridium centers). Similar observations of such a monohydrido-bridged iridium dinuclear system have been reported in the literature.[33] Intermediate **B** was found to be stable for ∼13 months when it was left under ambient conditions.

A mercury drop test confirmed that CO_2 was hydrogenated by a molecular pathway (Table 2), since addition of metallic mercury to the reaction contents did not inhibit the transformation of CO_2. As such, a plausible reaction mechanism involving **4** as a catalyst precursor is indicated in Scheme 3. In the presence of a base and water, **4** undergoes an aquation reaction. This results in the chloro ligand being replaced with a water ligand to give **6** (Scheme 2).

In the presence of H_2, **6** (which potentially exists in equilibrium with intermediate **A**) is converted to the hydrido-bridged iridium dinuclear species **B**. This step is probably followed by addition of a second mole of H_2 in the presence of a base, leading to intermediate **C** (**7**). However, with the presence of carbonate ions in aqueous solution, formation of the hydrido complex **C** might also be achieved by a bicarbonate- or water-assisted H_2 heterolysis.[19] It appears that although N-2 is electron-rich (Figure 2), this is not sufficient for it to act as a proton-responsive group that results in high TON in the range that was observed by Himeda and co-workers.[26] This is evidenced from optimizations of the solvent and base, for which higher TONs were obtained when a water/carbonate mixture was used in comparison to other solvent/base mixtures.

It is interesting to note that, for most of these half-sandwich iridium(III) catalytic systems, it has been proven by either experiments or computational calculations that CO_2 is the actual substrate undergoing reduction.[18,19] However, for the tetrazolylpyridyl catalytic systems, an alternative route toward formate formation is proposed. This route involves insertion of a bicarbonate ion into the iridium-hydride bond of **7**, yielding intermediate **D**. This can then be followed by loss of a hydroxyl group from **D** to afford intermediate **E**, which then subsequently reductively eliminates, resulting in expulsion of formate. Reactions of **7** with $NaHCO_3$, under CO_2 pressure and separately with CO_2 in the presence of NaOH, provided

Scheme 2. Formation of Catalytically Active Iridium Hydride Species

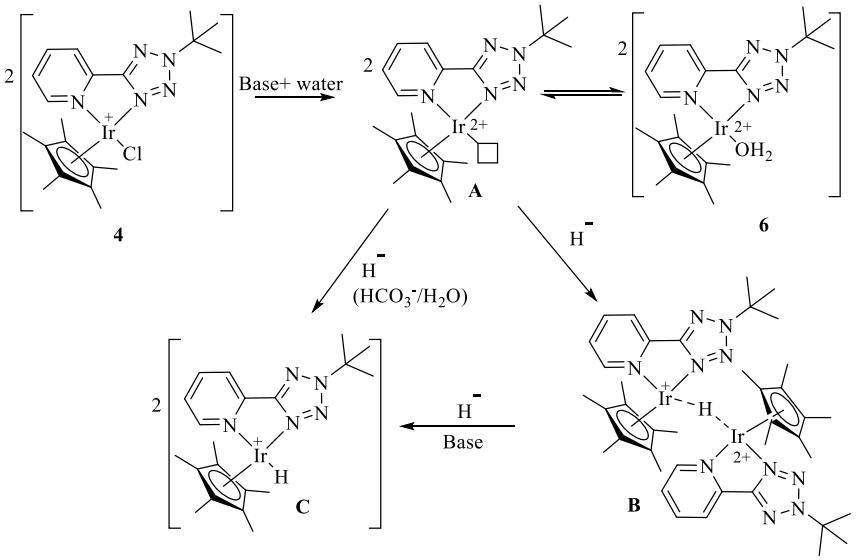

https://dx.doi.org/10.1021/acs.organomet.0c00276
Organometallics XXXX, XXX, XXX−XXX

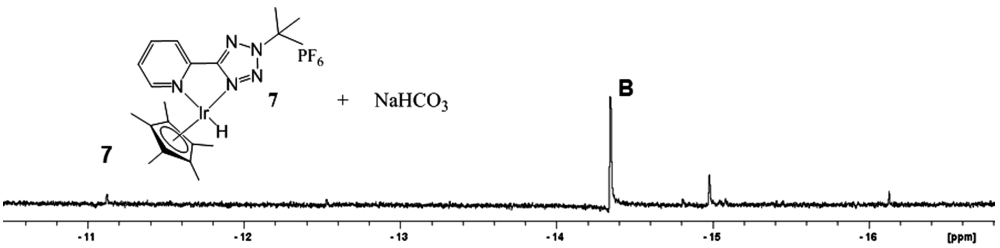

Figure 6. Investigation of the route of formation of iridium formato species by ^{1}H NMR spectroscopy. The reaction was performed in a high-pressure NMR tube; to 5 mg of **7** was added 10 mg of $NaHCO_3$ in 0.5 mL dmso-d_6 and the reaction monitored over time.

Scheme 3. Plausible Reaction Mechanism of N^N Bidentate Iridium Complexes for the CO_2 Hydrogenation Reaction

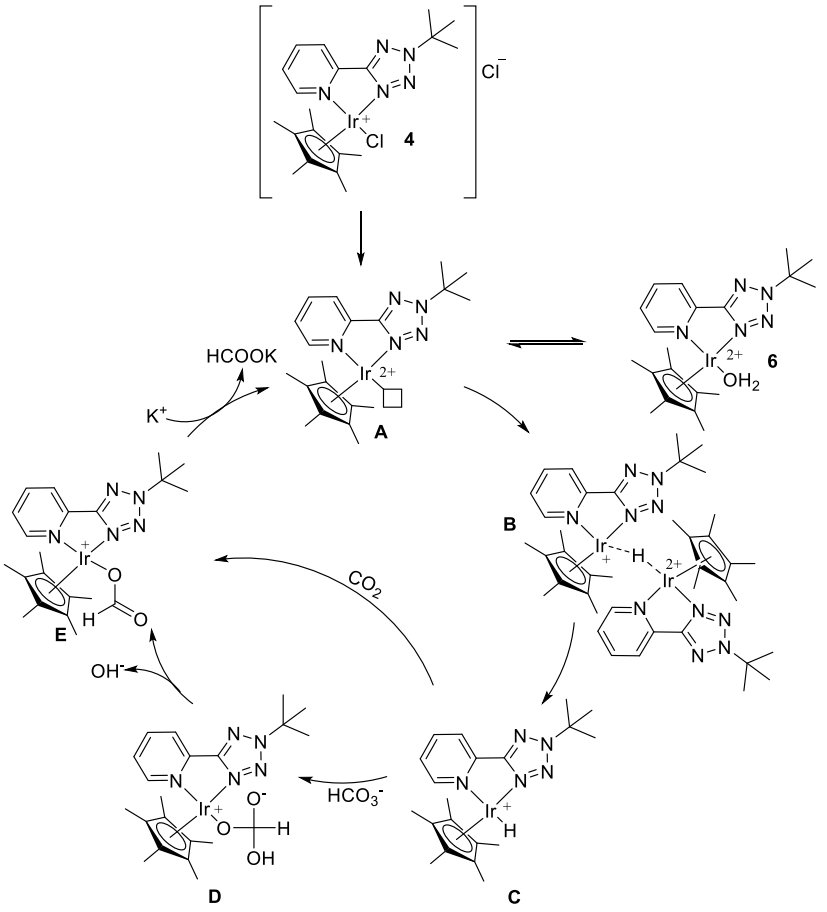

valuable insights into the actual hydrogenation step leading to the formation of the iridium formato species **E** (Figure 6).

The reaction of **7** with $NaHCO_3$ over a period of 3 h showed a gradual disappearance of the hydride peak of complex **7** (at −11 ppm) with the formation of a new iridium species with peaks at around −15 and −16 ppm. On consideration of the very low chemical shifts at which these peaks appear, they are likely to be due to an iridium hydride bicarbonate species that is bridged by a hydride or possibly species **D**, as indicated in Scheme 3.

Similar peaks were observed when a combination of CO_2 and NaOH was reacted with **7** (Figure 7). This is possibly as a result of the *in situ* formation of bicarbonate species from a basic aqueous CO_2 mixture. However, in the absence of a base, there seems to be no CO_2 insertion into the metal−hydride bond. This is in contrast to reported cases of various N^N bidentate iridium hydride systems.[5,19] However, such direct CO_2 insertion in the metal−hydride bond cannot be completely ruled out, as hydrogenating CO_2 in the presence of Et_3N resulted in formate production. As observed from the *in situ* ^{1}H NMR experiments, there is no reaction between **B** and $NaHCO_3$, CO_2, or a mixture of CO_2 + NaOH, since the peak at ∼−14 ppm remains over the course of the reaction. This indicates that **7** is the catalytically active species for the CO_2 hydrogenation reaction. Finally, in the last step of the reaction, the formate is expelled from the iridium formato **E** and further stabilized by K^+ ions while **A** is regenerated. In attempts to isolate the formato species **E**, iridium hydride **7** was reacted with excess $NaHCO_3$ at 70 °C for 16 h. Over the course of the reaction, **7**, which is not soluble in water, gradually dissolves in water, resulting in a yellow solution. The ^{1}H NMR spectrum of this reaction solution (Figure SI-6) showed the disappearance of the hydride peak accompanied by the appearance of a new formate peak at ∼8.4 ppm. However,

https://dx.doi.org/10.1021/acs.organomet.0c00276
Organometallics XXXX, XXX, XXX−XXX

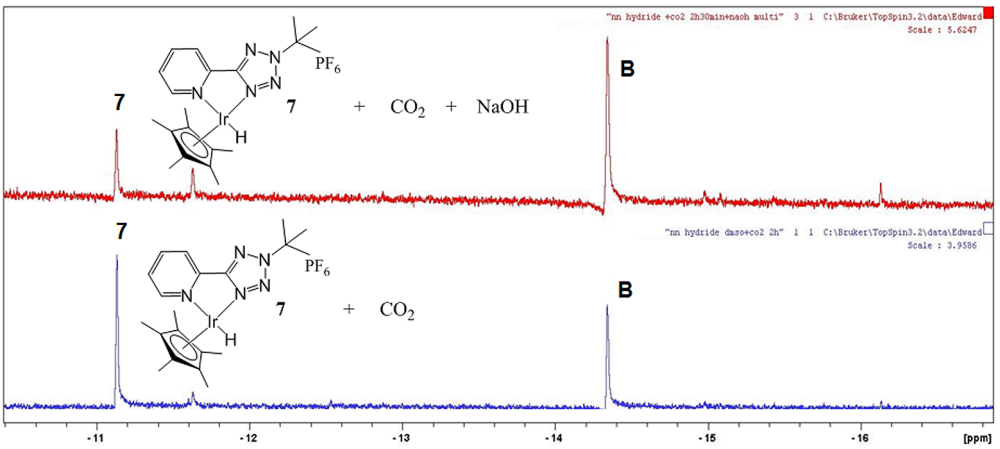

Figure 7. Investigation of the direct CO_2 insertion route for the formation of iridium formato species by ^1H NMR spectroscopy. (blue spectrum) The reaction was performed in a high-pressure NMR tube; to 5 mg of **7** in 0.5 mL of dmso-d_6 was added 50 bar of CO_2 and the reaction monitored over time. (red spectrum) The reaction was performed in a high-pressure NMR tube; to 5 mg of **7** in 0.5 mL of dmso-d_6 were added 5 mg of NaOH and 50 bar of CO_2 and the reaction was monitored over time.

a variety of ^1H NMR signals were observed, and this could be as a result of the formation of iridium aqua/hydroxyl species.

CONCLUSION

Two tetrazole-containing ligands and five tetrazole-containing iridium(III) and palladium(II) complexes have been synthesized and characterized using NMR spectroscopy, mass spectrometry, and infrared spectroscopy and in addition using single-crystal X-ray diffraction for complex **4**. The complexes were evaluated for their catalytic activity in CO_2 hydrogenation, for which there were varying degrees of success. The highest TON achieved was 560, which is significantly lower than those of other iridium(III) half-sandwich catalytic systems previously reported, therefore implying that the N2 position of the tetrazolyl ligand in the current systems is poorly proton responsive. Nonetheless, the iridium precatalysts were found to be more active in comparison to the palladium variant. The complexes were found to hydrogenate CO_2 in the presence of water via a homogeneous catalytic approach. The iridium precatalysts were observed to first undergo aquation in water. This was followed by formation of a bridging hydrido and a subsequent iridium hydride species. This iridium hydride species then goes on to hydrogenate bicarbonate species or CO_2 that was present in solution, yielding formate.

EXPERIMENTAL SECTION

All reactions were carried out in air unless otherwise stated. All solvents used were reagent grade, purchased from Sigma-Aldrich, and dried under nitrogen before use. 2-Cyanopyridine, sodium azide, triethylamine hydrochloride, *tert*-butyl alcohol, and 65% perchloric acid were purchased from Sigma-Aldrich and used without further purification. $PdCl_2$ and iridium(III) chloride were purchased from Heraeus (South Africa) and used as received. $[PdCl_2(MeCN)_2]$[34] and $[Ir(C_5Me_5)Cl_2]_2$[35] were synthesized according to literature procedures. NMR spectra were recorded on a Bruker 400 MHz NMR spectrometer (^1H at 400 MHz, $^{13}C\{^1H\}$ at 100 MHz, $^{13}P\{^1H\}$ NMR at 161.99 MHz). Spectrometer chemical shifts were reported relative to the internal standard tetramethylsilane (δ 0.00 ppm) and referenced to the residual proton and carbon signals at 7.24 and 77.0 ppm, respectively, of $CDCl_3$. Infrared spectra were obtained neat using a PerkinElmer Spectrum BX II spectrometer fitted with an ATR probe. Melting points were obtained using a Gallenkamp 5A 6797 digital melting-point apparatus. Elemental analysis was performed on a Thermos Scientific FLASH 2000 CHNS-O Analyzer. Mass spectrometry was performed using a Waters Synapt G2 mass spectrometer with both ESI positive and cone voltage 15 V. XRD spectra were obtained with a Bruker APEX-II CCD diffractometer.

Synthesis of 2-(2*H*-Tetrazol-5-yl)pyridine (1). Into a round-bottom flask containing 100 mL of toluene were placed 5.20 g (50 mmol) of 2-cyanopyridine, 4.2 g (65 mmol) of NaN_3, and 20.6 g (150 mmol) of $Et_3N{\cdot}HCl$, and the mixture was stirred at 110 °C for 24 h. After the reaction mixture was cooled to room temperature, 36% HCl was added until the mixture was acidic (pH 2) to precipitate the crude product. The mixture was then filtered, and the residue was washed with 36% HCl. The solid residue was then oven-dried for 20 min at 110 °C. The crude product was purified by dissolving in methanol followed by filtration and drying of the filtrate. Appearance: brown solid (yield 6.1 g, 83%). Solubility: soluble in water, methanol, and DMSO. ^1H NMR (400 MHz, DMSO, 30 °C) (ppm): 8.80 (d, ^3J = 4.4 Hz, 1H, H_{arom}), 8.23 (d, ^3J = 8.0 Hz, 1H, H_{arom}), 8.09 (t, ^3J = 6.4 Hz, 1H, H_{arom}), 7.66 (t, ^3J = 5.2 Hz, 1H, H_{arom}). $^{13}C\{^1H\}$ NMR (100.6 MHz, DMSO-d_6): 155.26; 150.53; 144.14; 138.71; 126.58; 123.08. Anal. Calcd for $C_6H_5N_5$: C, 48.98; H, 3.43; N, 47.60. Found: C, 48.78; H, 3.30; N, 47.44.

Synthesis of 2-(2-(*tert*-Butyl)-2*H*-tetrazol-5-yl)pyridine (2). In a round-bottom flask, *tert*-butyl alcohol (0.32 mL, 3.5 mmol) was slowly added to a suspension of 0.515 g of 2-(2*H*-tetrazol-5-yl)pyridine (**1**; 3.5 mmol) in 1.25 mL of 65% perchloric acid with stirring. The mixture was then stirred for 2 h at room temperature, after which 10 mL of 10 M NaOH was added. The aqueous mixture was then extracted with 3 × 25 mL portions of chloroform and dried *in vacuo* to yield **2**. Appearance: white solid (yield 0.55 g, 77%). Solubility: soluble in methanol, chloroform, and DMSO. ^1H NMR (400 MHz, $CDCl_3$, 30 °C) (ppm): 8.77 (d, ^3J = 4 Hz, 1H, H_{arom}), 8.25 (d, ^3J = 7.6 Hz, 1H, H_{arom}), 7.82 (t, ^3J = 1.6 Hz, 1H, H_{arom}), 7.36 (t, ^3J = 4.8 Hz, 1H, H_{arom}), 1.80 (s, 9H, H^t_{Bu}). $^{13}C\{^1H\}$ NMR (100.6 MHz, DMSO): 164.18; 150.56; 146.91; 138.03; 125.61; 122.81; 64.69; 29.31. Anal. Calcd for $C_{10}H_{13}N_5$: C, 59.10; H, 6.45; N, 34.46. Found: C, 59.22; H, 6.30; N, 34.44.

Synthesis of [$PdCl_2$(1)] (3). Into a Schlenk tube containing 10 mL of CH_2Cl_2 were placed 100 mg (0.67 mmol) of 2-(2*H*-tetrazol-5-yl)pyridine (**1**) and 176 mg (0.67 mmol) of $[PdCl_2(MeCN)_2]$. The reaction mixture was then stirred for 24 h at room temperature. After the reaction time had elapsed, the solvent was reduced *in vacuo* to yield the product. Appearance: brown solid (yield 176 mg, 81%). Solubility: soluble in DMSO. ^1H NMR (400 MHz, DMSO-d_6, 30 °C) (ppm): 8.98 (d, ^3J = 5.6 Hz, 1H, H_{arom}), 8.22 (t, ^3J = 7.6 Hz, 1H, H_{arom}), 8.11 (d, ^3J = 6.8 Hz, 1H, H_{arom}), 7.67 (t, ^3J = 6.8 Hz, 1H, H_{arom}). HR-ESI-MS: m/z $[M - N_2]^+$ 293.0515. Anal. Calcd for

https://dx.doi.org/10.1021/acs.organomet.0c00276
Organometallics XXXX, XXX, XXX−XXX

$C_6H_5N_5PdCl_2$: C, 22.21; H, 1.55; N, 21.59. Found: C, 22.51; H, 1.11; N, 21.77.

Synthesis of [IrCp*Cl(2)]Cl$^-$ (4). Into a Schlenk tube containing 5 mL of CH_2Cl_2 were placed 200 mg (0.98 mmol) of 2-(2-(*tert*-butyl)-2*H*-tetrazol-5-yl)pyridine (**2**) and 388 mg (0.49 mmol) of $[Ir(C_5Me_5)Cl_2]_2$. The reaction mixture was then stirred for 24 h at room temperature. After the reaction time had elapsed, the solvent was reduced *in vacuo* to yield the product. Appearance: yellow solid (yield 545 mg, 93%). Solubility: soluble in DCM and $CHCl_3$. ^{1}H NMR (400 MHz, $CDCl_3$, 30 °C) (ppm): 9.10 (d, ^3J = 5.2 Hz, 1H, H_{arom}), 8.35 (m, 2H, H_{arom}), 8.11 (t, ^3J = 5.6 Hz, 1H, H_{arom}), 1.86 (s, 9H, H^tBu), 1.77 (s, 15H, H_{Cp}*). ^{13}C{^{1}H} NMR (100.6 MHz, DMSO): 165.81; 153.41; 142.74; 141.23; 131.30; 124.27; 89.90; 69.46; 29.33; 9.31. HR-ESI-MS: $[M]^+$ *m*/*z* 566.1660. Anal. Calcd for $C_{20}H_{28}Cl_2IrN_5$: C, 39.93; H, 4.69; N, 11.64. Found: C, 40.48; H, 4.30; N, 11.44.

Synthesis of [IrCp*SO$_4$(2)] (5). Into a Schlenk tube containing 5 mL of water was placed 20 mg (0.033 mmol) of **4** and the mixture stirred for 10 min followed by the addition of 10.37 mg (0.033 mmol) of Ag_2SO_4. The reaction mixture was then stirred for 16 h at 40 °C. After the reaction time had elapsed, the reaction mixture was filtered and the filtrate dried *in vacuo* to yield the product. Appearance: yellow solid (yield 18 mg, 87%). Solubility: soluble in water and $CHCl_3$. ^{1}H NMR (400 MHz, D_2O, 30 °C) (ppm): 9.06 (d, ^3J = 5.2 Hz, 1H, H_{arom}), 8.38 (d, ^3J = 7.6 Hz, 1H, H_{arom}), 8.29 (t, ^3J = 7.6 Hz, 1H, H_{arom}), 7.84 (t, ^3J = 6.0 Hz, 1H, H_{arom}), 1.77 (s, 9H, H^tBu), 1.63 (s, 15H, H_{Cp}*). ^{13}C{^{1}H} NMR (100.6 MHz, D_2O): 166.71; 152.76; 143.76; 142.41; 130.21; 124.34; 89.75; 69.92; 28.16; 8.86. HR-ESI-MS: $[M + H]^+$ *m*/*z* 628.1513. Anal. Calcd for $C_{20}H_{28}IrN_5O_4S$: C, 38.33; H, 4.50; N, 11.17. Found: C, 38.48; H, 4.77; N, 11.44.

Synthesis of [IrCp*H$_2$O(2)](PF$_6$)$_2$ (6). Into a Schlenk tube containing 5 mL of water was placed 27 mg (0.043 mmol) of **5** and the mixture stirred for 10 min followed by the addition of 14.47 mg (0.086 mmol) of $NaPF_6$. The reaction mixture was then stirred for 30 min at room temperature. After the reaction time had elapsed, the reaction mixture was filtered. To the residue was added 15 mL of methanol, and the resulting suspension was filtered. Drying this filtrate *in vacuo* for 6 h yielded the desired product. Appearance: yellow solid (yield 31 mg, 86%). Solubility: soluble in methanol and insoluble in water and $CHCl_3$. ^{1}H NMR (400 MHz, MeOD, 30 °C) (ppm): 9.30 (d, ^3J = 5.6 Hz, 1H, H_{arom}), 8.61 (d, ^3J = 7.6 Hz, 1H, H_{arom}), 8.52 (t, ^3J = 8.0 Hz, 1H, H_{arom}), 8.09 (t, ^3J = 6.0 Hz, 1H, H_{arom}), 1.97 (s, 9H, H^tBu), 1.82 (s, 15H, H_{Cp}*). ^{13}C{^{1}H} NMR (100.6 MHz, D_2O): 152.95; 142.61; 141.27; 130.39; 124.87; 124.11; 90.40; 90.22; 27.87; 7.62. HR-ESI-MS: $[M]^+$ *m*/*z* 550.1962. Anal. Calcd for $C_{20}H_{30}F_{12}IrN_5OP_2$: C, 28.64; H, 3.61; N, 8.35. Found C, 28.48; H, 3.77; N, 8.44.

Synthesis of [IrCp*H(2)](PF$_6$) (7). Into a Schlenk tube containing 5 mL of water was placed 20 mg (0.0319 mmol) of **5** and the mixture stirred for 10 min. This was followed by the addition of 867.76 mg (12.76 mmol) of HCOONa, and the mixture was heated at 70 °C for 30 min. KPF_6 (0.0587g, 0.0319 mmol) was then added to the reaction mixture, which was then stirred for 30 min at room temperature. After the reaction time had elapsed, the reaction mixture was filtered and the residue dried in an oven at 80 °C for 20 min to yield the desired product. Appearance: yellow solid (yield 18 mg, 83%). Solubility: soluble in DMSO and insoluble in water. ^{1}H NMR (400 MHz, DMSO, 30 °C) (ppm): 8.99 (d, ^3J = 5.6 Hz, 1H, H_{arom}), 8.50 (d, ^3J = 7.6 Hz, 1H, H_{arom}), 8.26 (t, ^3J = 7.2 Hz, 1H, H_{arom}), 7.79 (t, ^3J = 6.0 Hz, 1H, H_{arom}), 1.84 (s, 15H, H_{Cp}*), 1.77 (s, 9H, H^tBu), −11.12 (s, 1H, H_{IrH}). ^{13}C{^{1}H} NMR (100.6 MHz, DMSO): 155.88; 141.82; 141.22; 131.32; 125.27; 124.10; 90.80; 90.20; 28.07; 7.92. HR-ESI-MS: $[M]^+$ *m*/*z* 532.2062. Anal. Calcd for $C_{20}H_{29}F_6IrN_5P$: C, 35.50; H, 4.32; N, 10.35. Found: C, 35.88; H, 3.97; N, 10.44.

Isolation of Intermediate B. In a stainless steel reactor, 20 mg of **5** (0.03 mmol) was dissolved in 0.5 mL of DMSO-d_6. The reactor was pressurized with 5 bar of H_2 and the solution subsequently stirred at 100 °C for 1 h. After the reaction time had elapsed, the reactor was cooled and the gas vented out. The crude mixture was then dried at 90 °C under vacuum to remove the solvent. Appearance: yellowish brown solid (yield 15 mg, 75%). Solubility: soluble in DMSO and insoluble in chloroform, diethyl ether, and hexane. ^{1}H NMR (400 MHz, DMSO, 30 °C) (ppm): 8.76 (d, ^3J = 6.2 Hz, 2H, H_{arom}), 8.15 (d, ^3J = 7.6 Hz, 2H, H_{arom}), 8.02 (t, ^3J = 7.2 Hz, 2H, H_{arom}), 7.57 (t, ^3J = 6.2 Hz, 2H, H_{arom}), 1.98 (s, 30H, H_{Cp}*), 1.77 (s, 18H, H^tBu), −14.34 (s, 1H, $H_{Ir-H-Ir}$). ^{13}C{^{1}H} NMR (100.6 MHz, DMSO-d_6): 165.32; 154.66; 145.06; 142.40; 130.55; 124.64; 94.90; 69.85; 29.00; 8.55. HR-ESI-MS: $[M - 2CH_3]^+$ *m*/*z* 1032.27, $[M - N^tBu]^+$ *m*/*z* 993.26, $[M - N^tBu - {}^tBu]^+$ *m*/*z* 934.16. Anal. Calcd for $C_{40}H_{58}Ir_2N_{10}O_8S_2$: C, 38.27; H, 4.66; N, 11.16. Found: C, 38.62; H, 4.91; N, 11.44.

General CO_2 Hydrogenation Reaction. In a stainless steel reactor, an appropriate amount of the appropriate catalyst was dissolved in 10 mL of the appropriate solvent. A 3.55 mmol amount of the appropriate base was added and the resulting solution pressurized with the required CO_2/H_2 mixtures. The reaction mixture was then stirred at an appropriate temperature for the required time at 1500 rpm. After the appropriate reaction time had elapsed, the reactor was cooled and the gases were slowly vented. A 0.4 mL portion of the contents of the reactor was sampled and added to 0.2 mL of D_2O and 5 μL of DMF (as a standard). The amount of product (formate) obtained was calculated by integral relations between the singlet formate peak at 8.3 ppm and the singlet DMF formamide peak at 7.9 ppm in the ^{1}H NMR spectrum of the sample.

Experimental Description of Generating an Electrostatic Potential Map. Calculation was carried out with the Spartan 14 Molecular Modeling program (Wavefunction, 2014) at the semi-empirical PM6 level of theory. The starting geometry of the molecular system was constructed using the Spartan graphical model builder and minimized interactively using the sybyl force field. The geometry was fully optimized without any symmetry constraints. The optimized geometry was subjected to full frequency calculations to verify the nature of the stationary points. The equilibrium geometry was characterized by the absence of imaginary frequencies.

■ ASSOCIATED CONTENT

Supporting Information

The Supporting Information is available free of charge at https://pubs.acs.org/doi/10.1021/acs.organomet.0c00276.

^{1}H NMR and mass spectra of selected complexes and reactions as well as data for the optimization of reaction conditions (PDF)

Cartesian coordinates of the calculated structure (XYZ)

Spartan file for complex **4** (ZIP)

Accession Codes

CCDC 1935810 contains the supplementary crystallographic data for this paper. These data can be obtained free of charge via www.ccdc.cam.ac.uk/data_request/cif, or by emailing data_request@ccdc.cam.ac.uk, or by contacting The Cambridge Crystallographic Data Centre, 12 Union Road, Cambridge CB2 1EZ, UK; fax: +44 1223 336033.

■ AUTHOR INFORMATION

Corresponding Author

Banothile C. E. Makhubela − *Research Centre for Synthesis and Catalysis, Department of Chemical Sciences, University of Johannesburg, Auckland Park 2006, South Africa;* orcid.org/0000-0002-2292-7400; Email: bmakhubela@uj.ac.za

Authors

Edward Ocansey − *Research Centre for Synthesis and Catalysis, Department of Chemical Sciences, University of Johannesburg, Auckland Park 2006, South Africa;* orcid.org/0000-0002-6847-2915

https://dx.doi.org/10.1021/acs.organomet.0c00276
Organometallics XXXX, XXX, XXX−XXX

James Darkwa − *Research Centre for Synthesis and Catalysis, Department of Chemical Sciences, University of Johannesburg, Auckland Park 2006, South Africa*

Complete contact information is available at: https://pubs.acs.org/10.1021/acs.organomet.0c00276

Notes

The authors declare no competing financial interest.

■ ACKNOWLEDGMENTS

We acknowledge the National Research Foundation of South Africa (NRF) for financial assistance (Grant Nos. 117989 and 112943). We thank Sasol SA, the University of Johannesburg Centre for Synthesis and Catalysis, and the UJ Faculty of Science Spectrum for use of facilities. The authors also thank Dr. Gift Mehlana (Midlands State University, Zimbabwe) for his assistance in the solution of the crystal structure.

■ REFERENCES

(1) Kröcher, O.; Köppel, R. A.; Baiker, A. Highly Active Ruthenium Complexes with Bidentate Phosphine Ligands for the Solvent-Free Catalytic Synthesis of N,N-Dimethylformamide and Methyl Formate. *Chem. Commun.* **1997**, *2* (5), 453−454.

(2) Dayan, O.; Dayan, S.; Kani, I.; Çetinkaya, B. Ruthenium(II) Complexes Bearing Pyridine-Based Tridentate and Bidentate Ligands: Catalytic Activity for Transfer Hydrogenation of Aryl Ketones. *Appl. Organomet. Chem.* **2012**, *26* (12), 663−670.

(3) Sharma, A. K.; Joshi, H.; Sharma, K. N.; Gupta, P. L.; Singh, A. K. 2 - Propanol vs Glycerol as Hydrogen Source in Catalytic Activation of Transfer Hydrogenation with (η6-Benzene)Ruthenium-(II) Complexes of Unsymmetrical Bidentate Chalcogen Ligands. *Organometallics* **2014**, *33*, 3629−3639.

(4) Zeng, L.; Wu, F.; Li, Y. Y.; Dong, Z. R.; Gao, J. X. Synthesis and Characterization of Novel Chiral Bidentate P,N-Containing Ligands and Ruthenium(II) Complex. The Application in Asymmetric Transfer Hydrogenation of Ketones. *J. Organomet. Chem.* **2014**, *762* (II), 34−39.

(5) Inoue, Y.; Izumida, H.; Sasaki, Y.; Hashimoto, H. Catalytic fixation of carbon dioxide to formic acid by transition-metal complexes under mild conditions. *Chem. Lett.* **1976**, *5*, 863−864.

(6) Bertini, F.; Glatz, M.; Gorgas, N.; Stöger, B.; Peruzzini, M.; Veiros, L. F.; Kirchner, K. A.; Gonsalvi, L. Carbon Dioxide Hydrogenation Catalysed by Well- Defined Mn(I) PNP Pincer Hydride Complexes. *Chem. Sci.* **2017**, *8*, 5024−5029.

(7) Bertini, F.; Gorgas, N.; Stöger, B.; Peruzzini, M.; Veiros, L. F.; Kirchner, K. A.; Gonsalvi, L. Efficient and Mild Carbon Dioxide Hydrogenation to Formate Catalyzed by Fe(II)-Hydridocarbonyl Complexes Bearing 2, 6- (Diaminopyridyl) Diphosphine Pincer Ligands. *ACS Catal.* **2016**, *6* (5), 2889−2893.

(8) Weilhard, A.; Qadir, M. I.; Sans, V.; Dupont, J. Selective CO_2 Hydrogenation to Formic Acid with Multifunctional Ionic Liquids. *ACS Catal.* **2018**, *8* (3), 1628−1634.

(9) Grossman, O.; Azerraf, C.; Gelman, D. Palladium Complexes Bearing Novel Strongly Bent Trans-Spanning Diphosphine Ligands: Synthesis, Characterization, and Catalytic Activity. *Organometallics* **2006**, *25* (2), 375−381.

(10) Burgess, S. A.; Kendall, A. J.; Tyler, D. R.; Linehan, J. C.; Appel, A. M. Hydrogenation of CO_2 in Water Using a Bis(Diphosphine) Ni-H Complex. *ACS Catal.* **2017**, *7* (4), 3089−3096.

(11) Bays, J. T.; Priyadarshani, N.; Jeletic, M. S.; Hulley, E. B.; Miller, D. L.; Linehan, J. C.; Shaw, W. J. The Influence of the Second and Outer Coordination Spheres on $Rh(Diphosphine)_2$ CO_2 Hydrogenation Catalysts. *ACS Catal.* **2014**, *4*, 3663−3670.

(12) Langer, R.; Diskin-Posner, Y.; Leitus, G.; Shimon, L. J. W.; Ben-David, Y.; Milstein, D. Low-Pressure Hydrogenation of Carbon Dioxide Catalyzed by an Iron Pincer Complex Exhibiting Noble Metal Activity. *Angew. Chem., Int. Ed.* **2011**, *50*, 9948−9952.

(13) Tanaka, R.; Yamashita, M.; Nozaki, K. Catalytic Hydrogenation of Carbon Dioxide Using Ir(III)-Pincer Complexes. *J. Am. Chem. Soc.* **2009**, *131* (40), 14168−14169.

(14) Schmeier, T. J.; Dobereiner, G. E.; Crabtree, R. H.; Hazari, N. Secondary Coordination Sphere Interactions Facilitate the Insertion Step in an Iridium(III) CO_2 Reduction Catalyst. *J. Am. Chem. Soc.* **2011**, *133* (24), 9274−9277.

(15) Malaza, S. S. P.; Makhubela, B. C. E. Direct and Indirect CO_2 Hydrogenation Catalyzed by Ir(III), Rh(III), Ru(II), and Os(II) Half-Sandwich Complexes to Generate Formates and N,N-Diethylformamide. *J. CO_2 Util.* **2020**, *39*, 101149.

(16) Makuve, N.; Mehlana, G.; Tia, R.; Darkwa, J.; Makhubela, B. C. E. Hydrogenation of Carbon Dioxide to Formate by α-Diimine RuII, RhIII, IrIII Complexes as Catalyst Precursors. *J. Organomet. Chem.* **2019**, *899*, 120892.

(17) Himeda, Y.; Onozawa-Komatsuzaki, N.; Sugihara, H.; Arakawa, H.; Kasuga, K. Transfer Hydrogenation of a Variety of Ketones Catalyzed by Rhodium Complexes in Aqueous Solution and Their Application to Asymmetric Reduction Using Chiral Schiff Base Ligands. *J. Mol. Catal. A: Chem.* **2003**, *195*, 95−100.

(18) Wang, W.-H.; Hull, J. F.; Muckerman, J. T.; Fujita, E.; Himeda, Y. Second-Coordination-Sphere and Electronic Effects Enhance Iridium(III)-Catalyzed Homogeneous Hydrogenation of Carbon Dioxide in Water near Ambient Temperature and Pressure. *Energy Environ. Sci.* **2012**, *5* (7), 7923−7926.

(19) Suna, Y.; Himeda, Y.; Fujita, E.; Muckerman, J. T.; Ertem, M. Z. Iridium Complexes with Proton-Responsive Azole-Type Ligands as Effective Catalysts for CO_2 Hydrogenation. *ChemSusChem* **2017**, *10* (22), 4535−4543.

(20) Li, X. Y.; Yin, Z.; Ma, W. M.; Wang, C.; Yu, Y. N.; Cheng, Y. Aperiodic Chemical Sequence in a Rod-Spacer Metal-Organic Framework from Linear Tetrazole-Benzene-Carboxylate Linker. *Inorg. Chem. Commun.* **2020**, *116*, 107925.

(21) Koren, P. N.; Gaponik, V. A.; Ostrovskii, O. Reactions of Azolium Cations. I. Kinetics and Mechanism of Alkylation of 5-phenyltetrazole with Isopropyl Alcohol in Aqueous Sulfuric Acid Media. *Int. J. Chem. Kinet.* **1993**, *25*, 1043−1051.

(22) Mosalkova, A. P.; Voitekhovich, S. V.; Lyakhov, A. S.; Ivashkevich, L. S.; Lach, J.; Kersting, B.; Gaponik, P. N.; Ivashkevich, O. A. 2-Tert-Butyl-5-(2-Pyridyl)-2H-Tetrazole as a Chelating Ligand in the Direct Synthesis of Novel Cu(II) and Heterobimetallic Cu(II)/Mn(II) Complexes. *Dalt. Trans.* **2013**, *42* (8), 2985−2997.

(23) Downard, A. J.; Peter, J.; Steenwijka, J. Syntheses of Chelating Tetrazole-Containing Ligands and Studies of Their Palladium(II) and Ruthenium(II) Complexes. *Aust. J. Chem.* **1995**, *48*, 1625−1642.

(24) Himeda, Y.; Onozawa-Komatsuzaki, N.; Miyazawa, S.; Sugihara, H.; Hirose, T.; Kasuga, K. $_P$H-Dependent Catalytic Activity and Chemoselectivity in Transfer Hydrogenation Catalyzed by Iridium Complex with 4,4'-Dihydroxy-2,2'- Bipyridine. *Chem. - Eur. J.* **2008**, *14* (35), 11076−11081.

(25) Wang, S.; Huang, H.; Dorcet, V.; Roisnel, T.; Bruneau, C.; Cedric, F. Efficient Iridium Catalysts for Base-Free Hydrogenation of Levulinic Acid Table of Contents. *Organometallics* **2017**, *36* (16), 3152−3162.

(26) Kanega, R.; Onishi, N.; Szalda, D. J.; Ertem, M. Z.; Muckerman, J. T.; Fujita, E.; Himeda, Y. CO_2 Hydrogenation Catalysts with Deprotonated Picolinamide Ligands. *ACS Catal.* **2017**, *7* (10), 6426−6429.

(27) Siek, S.; Burks, D. B.; Gerlach, D. L.; Liang, G.; Tesh, J. M.; Thompson, C. R.; Qu, F.; Shankwitz, J. E.; Vasquez, R. M.; Chambers, N.; Szulczewski, G. J.; Grotjahn, D. B.; Webster, C. E.; Papish, E. T. Iridium and Ruthenium Complexes of N-Heterocyclic Carbene- and Pyridinol-Derived Chelates as Catalysts for Aqueous Carbon Dioxide Hydrogenation and Formic Acid Dehydrogenation: The Role of the Alkali Metal. *Organometallics* **2017**, *36* (6), 1091−1106.

(28) Gunasekar, G. H.; Yoon, Y.; Baek, I. H.; Yoon, S. Catalytic Reactivity of an Iridium Complex with a Proton Responsive N-Donor

Ligand in CO_2 Hydrogenation to Formate. *RSC Adv.* **2018**, *8* (3), 1346−1350.
(29) Himeda, Y. Highly Efficient Hydrogen Evolution by Decomposition of Formic Acid Using an Iridium Catalyst with 4,4'-Dihydroxy-2,2'-Bipyridine. *Green Chem.* **2009**, *11* (12), 2018−2022.
(30) Tenno, T.; Rikmann, E.; Zekker, I.; Tenno, T.; Daija, L.; Mashirin, A. Modelling Equilibrium Distribution of Carbonaceous Ions and Molecules in a Heterogeneous System of $CaCO_3$-Water-Gas. *Proc. Est. Acad. Sci.* **2016**, *65* (1), 68.
(31) Brewster, T. P.; Miller, A. J. M.; Heinekey, D. M.; Goldberg, K. I. Hydrogenation of Carboxylic Acids Catalyzed by Half-Sandwich Complexes of Iridium and Rhodium. *J. Am. Chem. Soc.* **2013**, *135*, 16022−16025.
(32) Vogt, M.; Pons, V.; Heinekey, D. M. Synthesis and Characterization of a Dicationic Dihydrogen Complex of Iridium with a Bis-Carbene Ligand Set. *Organometallics* **2005**, *24* (8), 1832−1836.
(33) Kashiwame, Y.; Kuwata, S.; Ikariya, T. Metal - Pyrazole Bifunction in Half-Sandwich C-N Chelate Iridium Complexes: Pyrazole - Pyrazolato Interconversion and Application to Catalytic Intramolecular Hydroamination of Aminoalkene. *Chem. - Eur. J.* **2010**, *16*, 766−770.
(34) Anderson, G. K.; Lin, M.; Sen, A.; Gretz, E. *Bis(Benzonitrile) Dichloro Complexes of Palladium and Platinum*; Wiley: Hoboken, NJ, USA, 2007. DOI: DOI: 10.1002/9780470132593.ch13.
(35) White, A.; Yates, P. M.; Maitlis, C. (Pentamethylcyclopentadienyl)Rhodium and Iridium Compounds. In *Inorganic Syntheses*; Wiley Online Library: 1992; p 228.

https://dx.doi.org/10.1021/acs.organomet.0c00276
Organometallics XXXX, XXX, XXX−XXX